

Article

Future Climate Change Impact on the Nyabugogo Catchment Water Balance in Rwanda

Adeline Umugwaneza^{1,2,3}, Xi Chen^{1,2,*}, Tie Liu^{1,2} , Zhengyang Li^{1,2}, Solange Uwamahoro^{1,2}, Richard Mind'je^{1,2,3}, Edovia Dufatanye Umwali^{1,2,3}, Romaine Ingabire^{2,4} and Aline Uwineza⁵

- ¹ State Key Laboratory of Desert and Oasis Ecology, Xinjiang Institute of Ecology and Geography, Chinese Academy of Sciences, Urumqi 830011, China; umugwaneza15@hotmail.com (A.U.); liutie@ms.xjb.ac.cn (T.L.); lizhengyang19@mails.ucas.ac.cn (Z.L.); uwamahoroso@mails.ucas.ac.cn (S.U.); mindjerichard@mails.ucas.ac.cn (R.M.); umwariedovia@outlook.com (E.D.U.)
- ² University of Chinese Academy of Sciences, Beijing 100049, China; ingabireromaine@gmail.com
- ³ Faculty of Environmental Sciences, University of Lay Adventists of Kigali (UNILAK), Kigali P.O. Box 6392, Rwanda
- ⁴ Center for Agricultural Resources Research, Institute of Genetics and Developmental Biology, Chinese Academy of Sciences, Shijiazhuang 050022, China
- ⁵ Faculty of Engineering, University of Miyazaki, Miyazaki 889-2192, Japan; alynuwineza@gmail.com
- * Correspondence: chenxi@ms.xjb.ac.cn

Abstract: Droughts and floods are common in tropical regions, including Rwanda, and are likely to be aggravated by climate change. Consequently, assessing the effects of climate change on hydrological systems has become critical. The goal of this study is to analyze the impact of climate change on the water balance in the Nyabugogo catchment by downscaling 10 global climate models (GCMs) from CMIP6 using the inverse distance weighting (IDW) method. To apply climate change signals under the Shared Socioeconomic Pathways (SSPs) (low and high emission) scenarios, the Soil and Water Assessment Tool (SWAT) model was used. For the baseline scenario, the period 1950–2014 was employed, whereas the periods 2020–2050 and 2050–2100 were used for future scenario analysis. The streamflow was projected to decrease by 7.2 and 3.49% under SSP126 in the 2020–2050 and 2050–2100 periods, respectively; under SSP585, it showed a 3.26% increase in 2020–2050 and a 4.53% decrease in 2050–2100. The average annual surface runoff was projected to decrease by 11.66 (4.40)% under SSP126 in the 2020–2050 (2050–2100) period, while an increase of 3.25% in 2020–2050 and a decline of 5.42% in 2050–2100 were expected under SSP585. Climate change is expected to have an impact on the components of the hydrological cycle (such as streamflow and surface runoff). This situation may, therefore, lead to an increase in water stress, calling for the integrated management of available water resources in order to match the increasing water demand in the study area. This study's findings could be useful for the establishment of adaptation plans to climate change, managing water resources, and water engineering.

Keywords: climate change; CMIP6; Nyabugogo catchment; Rwanda; SWAT model



Citation: Umugwaneza, A.; Chen, X.; Liu, T.; Li, Z.; Uwamahoro, S.; Mind'je, R.; Dufatanye Umwali, E.; Ingabire, R.; Uwineza, A. Future Climate Change Impact on the Nyabugogo Catchment Water Balance in Rwanda. *Water* **2021**, *13*, 3636. <https://doi.org/10.3390/w13243636>

Academic Editor: Hongbo Ling

Received: 20 October 2021

Accepted: 13 December 2021

Published: 17 December 2021

Publisher's Note: MDPI stays neutral with regard to jurisdictional claims in published maps and institutional affiliations.



Copyright: © 2021 by the authors. Licensee MDPI, Basel, Switzerland. This article is an open access article distributed under the terms and conditions of the Creative Commons Attribution (CC BY) license (<https://creativecommons.org/licenses/by/4.0/>).

1. Introduction

Globally, climate change is becoming one of the most significant barriers to achieving food, energy, and water security. The impact is particularly severe in developing nations, due to their limited adaptive capacity and inadequate environmental resource management [1]. Moreover, the hydrological cycle is predicted to become more intense as a result of global warming, leading to more frequent floods and droughts, which will have an impact on ecosystem services and water resources [2]. Changes in precipitation patterns have a direct impact on water availability and runoff, whereas evapotranspiration is affected by changes in temperature, radiation, and humidity [3,4]. Previous works have confirmed that climate change is expected to cause alterations in precipitation patterns, variation in the frequency and distribution of droughts and floods, and intensification of

the evapotranspiration rates in different regions worldwide [5,6]. Under climate change scenarios, streamflow variations have been depicted as being associated with variations in precipitation [7]. However, for moisture-scarce regions, a small increase in temperature and the related increase in evapotranspiration can instigate huge changes in streamflow [8].

To achieve the Sustainable Development Goals (SDGs), it is important to assess future water resource conditions under projected climate change in order to develop better water management systems and climate adaptation strategies [9]. However, several studies around the world have estimated the impact of climate change on streamflow using different hydrological models and climate scenarios [10,11]. Commonly, these studies indicated that climate change would have a significant impact on the availability of water resources around the world.

Africa is one of the most sensitive regions to climatic variability, due to its high exposure and insufficient adaptability [12]. The Intergovernmental Panel on Climate Change (IPCC) reported that developing nations are more vulnerable to climate change and its consequences due to their economic, climatic, and geographic conditions. According to the IPCC [13], the population of Africa under danger of rising water stress is predicted to reach 75–250 million and 350–600 million by the 2020s and 2050s, respectively. Furthermore, yields from rain-fed agriculture could be reduced by up to 50% in rain-fed-agriculture-dependent nations such as Rwanda. Numerous studies concur that the climate patterns of the continent are changing [14–16]. For instance, Adhikari, et al. [1] reviewed the impacts of population growth and climate change on water resources across eight East African countries, including Rwanda, and found that the majority of those countries are already water-stressed, or are on the verge of becoming so. Furthermore, the studies conducted by the authors of [17,18] argued that the projected increase in temperature is stable across the East African region, while precipitation projections are still more uncertain and variable. In Rwanda, previous studies assessed the impact of climate change on flooding using the Coupled Model Intercomparison Project Phase Three (CMIP3) [19,20], while Austin, et al. [21] focused on the impact of climate change on crops and their adaptation. Another recent study evaluated the performance of 10 CORDEX historical climate models against observed rainfall in Rwanda [22].

Nyabugogo is one of the most vulnerable catchments to climate variability in the region [23]. An increasing number of extreme hydrological events have affected the catchment, with significant consequences for the water supply system. Due to a lack of adaptive capacity, droughts and floods have become more frequent and intense, worsening food insecurity in the already susceptible zone [20,21]. However, no impact studies have synthetically used the latest CMIP6 to assess the hydrological responses to future climate change in the Nyabugogo catchment area, yet social and economic losses can be minimized by applying a mitigation approach and adaptation strategies. Therefore, the understanding of the problem caused by climate change in this catchment needs to be improved and updated.

In the current management of water resources, hydrological models play a vital role [24]. By integrating the anticipated future scenarios based on downscaled global climate model (GCM) data into hydrological models, the hydrological effects of climate change at the basin scale can be assessed [25]. Various hydrological models—including the Soil and Water Assessment Tool (SWAT), variable infiltration capacity (VIC), and MIKE SHE—have been applied to support the assessment of the impact of climate change on water resources under various environmental conditions and management techniques. With the advantage of having a lower number of input parameters compared to other modeling approaches, the SWAT is among the most popular models applied, and has proven its satisfactory accuracy in simulating the impact of climate change on different hydrological processes, in both long and short periods, under different climatic and soil conditions [25–27].

By evaluating the results from global climate models (GCMs) and employing the SWAT model for hydrological simulation, this study aims to examine the influence of climate change on the water balance in the Nyabugogo catchment under the Shared

Socioeconomic Pathways (SSPs). These SSP-based scenarios reflect future developments in the absence of climate change or new climate policies beyond those currently in place, as well as mitigation scenarios, which examine the effects of climate change mitigation policies on the baseline scenarios [28]. The specific objectives are (1) to downscale GCM outputs and predict the future climate in the Nyabugogo catchment under both low and high emissions scenarios—we used these to investigate and comprehend the hydrological impacts of the world’s fossil fuel emissions, as projected by these two scenarios; (2) to set up the SWAT model to represent the local hydrological processes; and (3) to analyze the influence of future climate change on water balance in the catchment. The results of the study will help to plan for hydrological structures such as dams and river diversions, and to develop sustainable site adaptation strategies that lessen the impact of climate change on agriculture, energy, and other sectors.

2. Materials and Methods

2.1. Study Area Description

The Nyabugogo catchment (Figure 1) is located in the central, eastern, and northern areas of Rwanda. The catchment area covers an area of 1661 km², and accounts for 6.31% of the total area of Rwanda. This catchment is rural, but is also mainly urbanized and densely populated. There is greater shale content in the western half of the study region, whereas the middle and east have mostly altered shale and quartzite by substantial granite, and pegmatite with alluvial material found at the valley’s bottom throughout the catchment. The most common soil types in the catchment are nitosol, acricol, alisol, and lixisol, with ferralsols in the drier eastern part near Lake Muhazi, and acricol in the western part, while camisole is also abundant in the western region. The catchment’s central part and valley bottom are defined by clay soils with low infiltration and a flat topography [29].

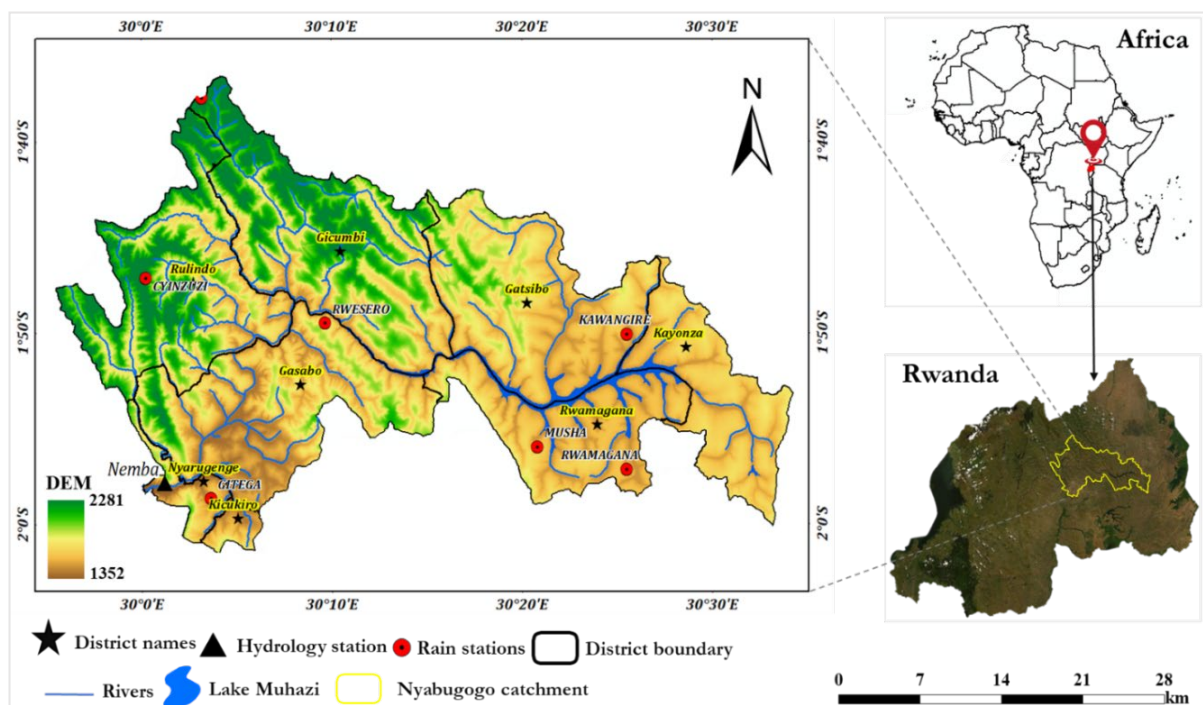


Figure 1. Location of Nyabugogo catchment in Rwanda.

The Nyabugogo catchment, similar to the rest of the country, has a temperate tropical climate, with mean annual precipitation ranging from 992 mm to 1128 mm, average annual evapotranspiration of 503 to 1050 mm [30], and temperatures ranging from 19 to 21°C [31]. Rwanda has two rainy and dry seasons. For rainy seasons, one is from the end of September to December, while the peak rainy season is from March to early May. The Nyabugogo River

flows through Kigali, and is fed by the Mwange, Muyanza, Rusine, Kajevuba, and Yanze rivers; it is 45.97 km long, measured from the outflow of Lake Muhazi to its confluence with the lower Nyabarongo River near Kigali at an elevation of ~1360 m above sea level. The highest point of the catchment is 2281 m above sea level in the northern part. The central feature of the catchment is Lake Muhazi, which is ~80 km long in the east–west [32,33]. Agriculture, fishing, and forestry are the most important employment sectors in the area, followed by trade and other services.

2.2. Data

The digital elevation model (DEM), land cover land use (LCLU) (Figure 2b), soil map (Figure 2a), and meteorological data are the main input data required for the ArcSWAT. A 30 m spatial resolution DEM from the Shuttle Radar Topography Mission (SRTM) was collected from the USGS Earth Explorer community (<http://www.dwtkns.com/srtm30m/> (accessed on 17 May 2020)) in order to acquire the topographic information on the study area, such as the overland slope and slope length for each delineated sub-basin. The land cover land use (LCLU) map was produced from a Landsat-8 Operational Land Imager (OLI) image (path/row: 172/61) obtained from the United States Geological Survey (USGS) through a global visualization tool. The soil texture was derived from the Digital Soil Map of the World (DSMW) (<http://www.fao.org/geonetwork/srv/en/metadata.show%3Fid=14116> (accessed on 14 January 2021) assembled by the United Nations Food and Agricultural Organization (FAO). Weather data from meteorological stations in the study area were provided by the Rwanda Meteorological Agency, while observed discharge data from Nemba Station (the outlet of the Nyabugogo catchment) were obtained from the Rwanda Water Resource Portal (<https://waterportal.rwb.rw/> (accessed on 11 December 2020)). Moreover, time series of rainfall and temperature data were collected from the Climate Research Unit (CRU) (<https://crudata.uea.ac.uk/cru/data/> (accessed on 30 April 2021) and presented at a high resolution (0.5° × 0.5° grids) for the period 1901–2014. This study used GCM datasets from the CMIP6 models.

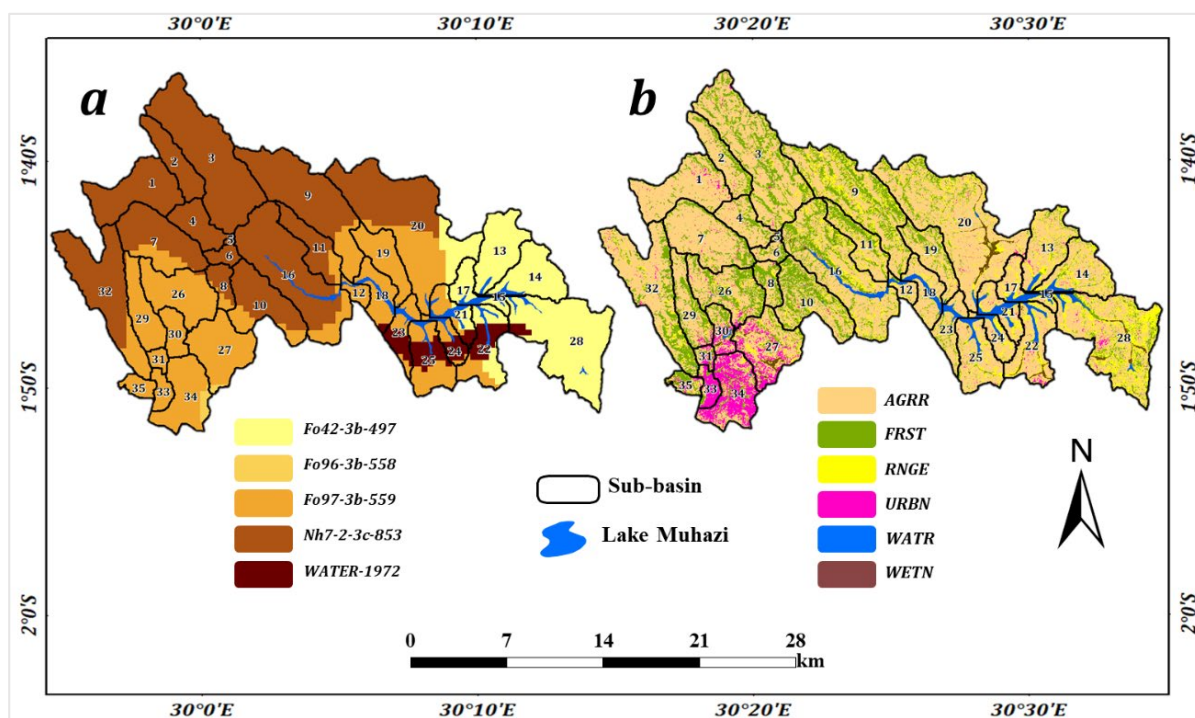


Figure 2. (a) Soil attributes and (b) land cover land use of the Nyabugogo catchment.

2.3. Methods

2.3.1. Description of the Stages Involved in the Study

The impact of climate change on water balance in the present study was evaluated in three stages: Firstly, the SWAT model was initially calibrated to simulate streamflow and runoff in the Nyabugogo catchment. Secondly, the GCM data were downscaled using the statistical downscaling model to reflect the future climate at the catchment level under the SSP126 (low emissions) and SSP585 (high emissions) scenarios. The observed data for the baseline period (1950–2014) were compared to the downscaled future climate. Finally, the calibrated and validated SWAT model was used to analyze the effects of future climate data on the water balance of the Nyabugogo catchment area, using the downscaled future climate data from the two emission scenarios.

2.3.2. SWAT Model

The SWAT model is a spatially distributed hydrological model that was designed to assist water resource managers in assessing the impacts of climate change, land use, and management approaches on water resources [34,35]. This model has been widely employed by researchers for watershed modeling and water resource management in watersheds with different climatic and topographic characteristics, owing to its user-friendly interface (ArcSWAT) and flexible data needs [27,36]; it has already been validated for various watershed scales in different climatic situations around the world, and it has worked well even in complex and data-poor watersheds [37]. The SWAT model also has the advantage of allowing the simulation of a variety of physical processes (e.g., hydrological, sediment, and contaminants) in a watershed. In the SWAT, the hydrological cycle of a sub-basin is simulated based on the following water balance equation:

$$SW_s = SW_o + \sum_{i=1}^n (R_{day} - Q_{surf} - E_a - W_{seep} - Q_{gw}) \quad (1)$$

where SW_s is the final soil water content, SW_o is the initial soil water content (mm), n is time, R_{day} is the amount of precipitation, Q_{surf} is the amount of surface runoff, E_a is the amount of evapotranspiration, W_{seep} is the amount of percolation flow exiting in the soil, and Q_{gw} is the amount of return flow.

DEM, LCLU, soil, and meteorological data are the core SWAT model inputs. The catchment is divided into physically connected sub-basins, which are further subdivided into hydrologic response units (HRUs). The HRUs are homogeneous entities with distinct land cover/use and soil characteristics. The catchment area was delineated into 35 sub-basins with 429 HRUs, each representing a distinct combination of land cover and soil type, in order to simplify the watershed and facilitate analysis. Weather data (daily rainfall and minimum and maximum temperature) were used to simulate streamflow and runoff. The soil conservation service (SCS) curve number approach was used to quantify surface runoff in the SWAT [38]. The Penman–Monteith, Hargreaves, and Priestley–Taylor techniques can all be used to calculate evapotranspiration (ET) in the hydrological SWAT model; however, we adopted the Hargreaves method to estimate ET in the Nyabugogo catchment [39,40]. This method uses the minimum and maximum daily temperatures as input data to estimate potential evapotranspiration [41,42]. The Hargreaves equation used in SWAT is expressed as:

$$ET = 0.0023 \times H_0 \times (T_{max} - T_{min})^{0.5} \times \left(\frac{T_{max} + T_{min}}{2} + 17.8 \right) \quad (2)$$

where ET is the evapotranspiration (mm d^{-1}), H_0 is the extraterrestrial radiation ($\text{MJ m}^{-2}\text{d}^{-1}$), and T_{max} and T_{min} are the maximum and minimum air temperatures for a given day ($^{\circ}\text{C}$), respectively.

Sensitivity Analysis, Model Calibration, Validation, and Evaluation

The SWAT model calibration and uncertainty program (SWAT-CUP) [43] was employed in this study to assess parameter sensitivity, uncertainty analysis, auto-calibration, and model validation. To determine the critical parameters (Table 1) that affect streamflow for calibration, the sensitivity analysis was performed using the Sequential Uncertainty Fitting (SUFI-2) algorithm [44]. Based on the global sensitivity analysis, the most sensitive input hydrological parameters were identified by the *t*-stat and *p*-value—the greater the absolute *t*-stat and the lower the *p*-value, the more sensitive the parameter. Manual calibration was carried out on the most sensitive parameters. The Nash–Sutcliffe efficiency (*NSE*), coefficient of determination (R^2), and relative error (*RE*) were applied to evaluate the model performance.

$$NSE = 1 - \frac{\sum_{i=1}^t (O_i - S_i)^2}{\sum_{i=1}^t (O_i - M_o)^2} \quad (3)$$

$$R^2 = \frac{\sum_{i=1}^t (O_i - M_o)(S_i - M_s)}{\left[\sum_{i=1}^t (O_i - M_o)^2 \right]^{0.5} \left[\sum_{i=1}^t (S_i - M_s)^2 \right]^{0.5}} \quad (4)$$

$$RE = \frac{|O_i - S_i|}{S_i} \times 100 \quad (5)$$

where O_i and S_i are the observed and simulated values, respectively, t is the total number of paired values, M_o is the mean observed value, and M_s is the mean simulated value.

Table 1. Parameters used for sensitivity analysis and calibration of the SWAT model.

Parameter Names	Description	Range	Fitting Value	<i>p</i> -Value	<i>t</i> -Stat (Absolute)
r_CN2.mgt	Curve number	−0.2–0.2	−0.1	0.00	22.48
r_SOL_AWC.sol	Available water capacity	0–1	0.25	0.01	1.61
r_ESCO.bsn	Soil evaporation compensation factor	0–1	0.5	0.01	1.47
r_SURLAG.bsn	Surface runoff lag time	1–24	3.5	0.04	0.99
v_REVAPMN.gw	Threshold water depth in the shallow aquifer for “revap”	0–1000	92.5	0.14	0.89
v_GW_REVAP.gw	Groundwater “revap” co-efficient	0.02–0.2	0.09	0.45	0.76
v_ALPHA_BF.gw	base flow alpha factor	0–1	0.23	0.47	0.72
v_GWQMN.gw	Threshold water depth in the shallow aquifer	0–5000	0.38	0.63	0.49
v_GW_DELAY.gw	Groundwater delay time	0–500	28	0.72	0.36
v_RCHRG_DP.gw	Recharge to deep aquifer	0–1	0.15	0.95	0.06

The prefix v means to multiply by original value, while r means to replace the original value.

2.3.3. Downscaling of Future Climate Scenarios

The Nyabugogo catchment was modeled using GCM data from the latest CMIP6 (Table 2) under SSP scenarios. This study examined the average growth rate of climate variables (precipitation and temperature) in the two periods of interest (2020–2050 and 2050–2100) relative to the baseline period (1950–2014). By 2100, the SSP1-2.6 (SSP5-8.5) represents a low number of (high energy-intensive) Shared Socioeconomic Pathways (SSPs), with a decline to 2.6 Wm^{-2} (rising to 8.5 Wm^{-2}) in radiation forcing [28,45]. As the spatial resolution of raw GCMs is generally too coarse for regional study, the statistical downscaling was performed before the application of future GCM projections into the calibrated SWAT. Using the inverse distance weighted (IDW) interpolation, these coarse-resolution anomalous fields of climate variables were interpolated to a 0.5-degree resolution. An ensemble modeling approach was then used to account for the uncertainties in the projected precipitation and temperatures [46,47]. The absolute or relative differences between the GCMs’ outputs for the baseline and future periods were computed for the data used in this study. The estimated changes were interpolated to high-resolution grids based on the assumption that climate change is relatively stable over space (high spatial

autocorrelation) [48]. Before being input into the SWAT model, changes were clustered into low, mean, and high ranks for each emission scenario, and for all considered runs that passed the performance evaluation. The low and high ranks correspond to the minimum and maximum values of the changes, respectively, and express the ranges of uncertainty associated with climate change. The mean rank corresponds to the mean values of the changes, and was considered to be reliable for hydrological impact simulation [49]. Daily time series for the SWAT model were generated using modeling results for daily maximum and minimum temperatures and mean precipitation from a multi-model ensemble of 10 GCM combinations under two scenarios. Overall, the CMIP6 with the SSP scenarios SSP126, and SSP585 was a projected output that was added to the baseline model of the catchment in order to assess climate change impacts.

Table 2. Detailed information of selected GCMs.

Model	Institute	Resolution	References
ACCESS-CM2	Commonwealth Scientific and Industrial Research Organization (CSIRO), Australia	1.25° × 1.87°	Bi, et al. [50]
ACCESS-ESM1-5	Commonwealth Scientific and Industrial Research Organization (CSIRO), Australia	1.25° × 1.87°	Law, et al. [51]
CNRM-CM6-1	CNRM (Centre National de Recherches Meteorologiques, Toulouse 31057, France), CERFACS (Centre Europeen de Recherche et de Formation Avancee en Calcul Scientifique, Toulouse 31057, France)	1.4° × 1.4°	Voltaire, et al. [52]
CNRM-ESM2-1	Centre National de Recherches Meteorologiques, Toulouse 31057, France Centre Europeen de Recherche et de Formation Avancee en Calcul Scientifique, France	1.4° × 1.4°	S��ferian, et al. [53]
CanESM5	Canadian Centre for Climate Modelling and Analysis, Environment and Climate Change Canada, Canada	2.8° × 2.8°	Swart, et al. [54]
INM-CM4-8	Marchuk Institute of Numerical Mathematics of The Russian Academy of Science	2° × 1.5°	Volodin, et al. [55]
INM-CM5-0	Marchuk Institute of Numerical Mathematics of The Russian Academy of Science	2° × 1.5°	Volodin, et al. [55]
IPSL-CM6A-LR	Institute Pierre Simon Laplace (IPSL), France	1.26° × 2.5°	Boucher, et al. [56]
MIROC6	Japan Agency for Marine-Earth Science and Technology (JAMSTEC), University of Tokyo (UT), National Institute for Environmental Studies (NIES), and RIKEN Center for Computational Science (RCCS), Japan	1.4° × 1.4°	Tatebe, et al. [57]
UKESM1-0-LL	Met Office Hadley Centre, UK	1.25° × 1.87°	[Sellar, et al. [58], Archibald, et al. [59]]

3. Results and Discussion

3.1. Climate Change Analysis

3.1.1. Projected Precipitation Change

This study quantifies the catchment's average future rainfall and temperature (1950–2014) in two time horizons—near future (2020–2050) and far future (2050–2100)—under two scenarios: SSP126 and SSP585. Figure 3a shows the relative changes in monthly rainfall under both scenarios and periods. We observed that the monthly rainfall would greatly increase in August and December by 8.84 and 7.08% per decade, respectively, under the SSP585 scenario in the 2050–2100 period, while a high decrease is expected in June under SSP126 in the 2020–2050 period. During the rain season, rainfall is projected to increase compared to dry season (Figure 3b). Similar to the findings of Almazroui, et al. [60] and Ongoma, et al. [61], in October, November, and December (OND) (Figure 3c), rainfall is projected to increase by 1.63–4.62% per decade under both scenarios and periods, while a decline is

projected in March, April, and May (MAM) in all scenarios and periods—consistent with a previous study [1]. The long rains (MAM) have been reported to be declining across most East African countries [17,47,62], despite global climate models predicting a wetter season. The rainfall is projected to increase in both scenarios and periods—mostly in the far-future period—which is consistent with the findings of Ayugi, et al. [47], whose results showed an increase in precipitation in the East African region. Using CMIP6, Almazroui, et al. [60] and Tan, et al. [63], reported that SSP126 will experience a lower change in rainfall than SSP585 in the Central East Africa region, while in both the near and long periods SSP126 is expected to have a lower change than SSP585. The findings of Ongoma, et al. [61] and Gebrechorkos, et al. [64] indicated that the projected rainfall would increase more under the high-emissions scenario than the low-emissions scenario using CMIP5.

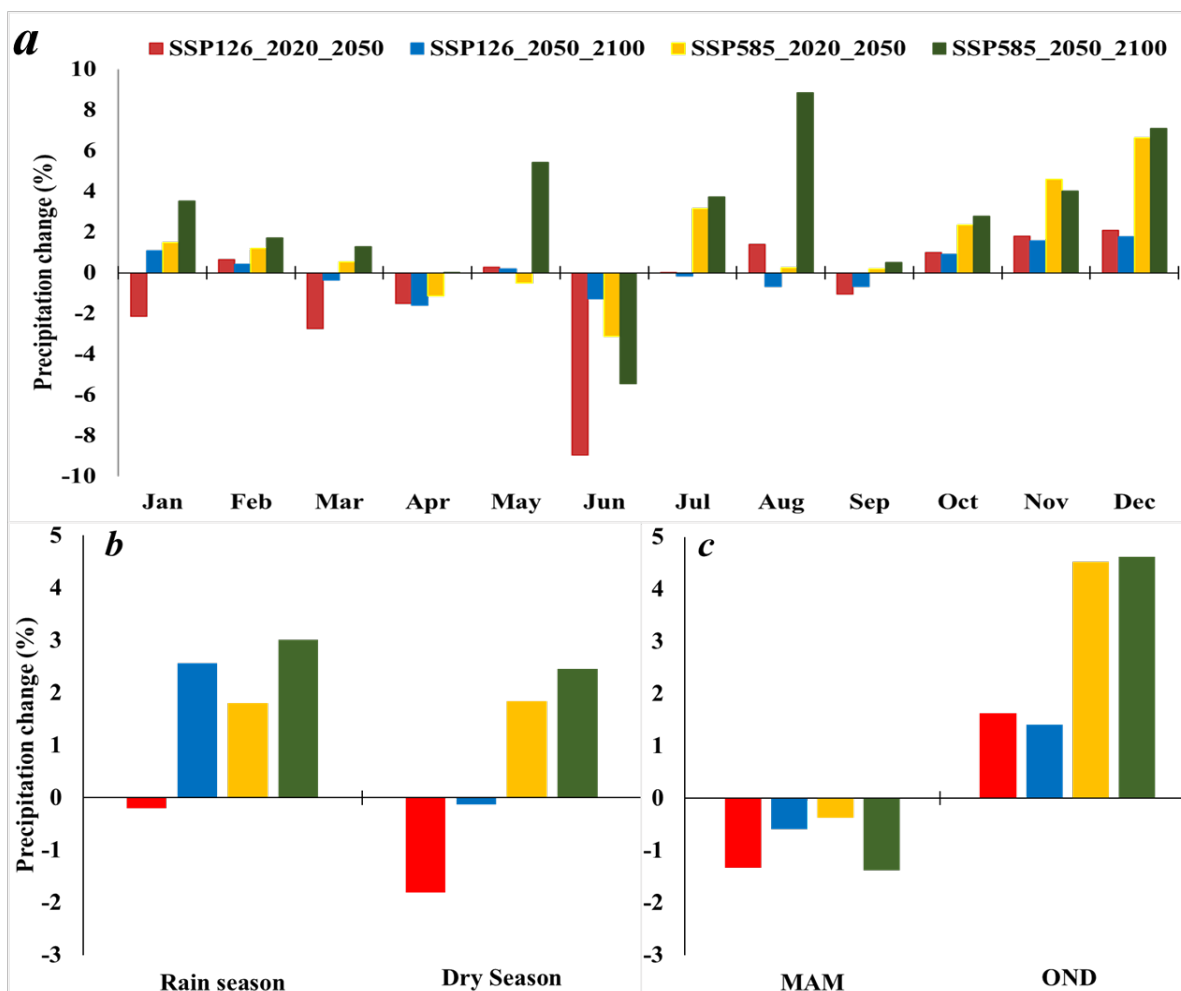


Figure 3. Relative precipitation changes: (a) monthly, (b) seasonal, and (c) in rainy seasons.

3.1.2. Projected Temperature Change

The projected temperature (minimum and maximum) is expected to rise in both scenarios for 2020–2050 and 2050–2100. For all periods (Figure 4), SSP585 showed a larger increase than SSP126. The rate of maximum temperature increase in May, June, July, August, and September is more than in the other months under both scenarios. A significant ($p < 0.05$) increase is observed under SSP585 during 2050–2100. In line with previous studies [18,65], the average annual minimum temperature is projected to increase by 0.27 and 0.20 °C decade⁻¹ under SSP126 during 2020–2050 and 2050–2100, respectively, with temperature projected to increase under SSP585 by 0.32 and 0.46 °C decade⁻¹ in 2020–2050 and 2050–2100, respectively. The average annual maximum temperature is

also expected to increase under both periods and scenarios (0.24 and 0.18 °C per decade, respectively) under SSP126 while under SSP585 it will increase by 0.27 and 0.41 °C per decade in 2020–2050 and 2050–2100, respectively. These findings are consistent with those of Engelbrecht, et al. [66], who found that under the high-emissions scenario, temperatures in the African tropics will rise by 3–5 °C from 2071 to 2100, compared to 1961–1990, using CMIP5 models. The maximum and minimum temperatures are projected to increase more in the dry season than in the wet season under both high and low emissions during the near- and far-future periods. This rising temperature is likely to have an impact on the increase in evapotranspiration.

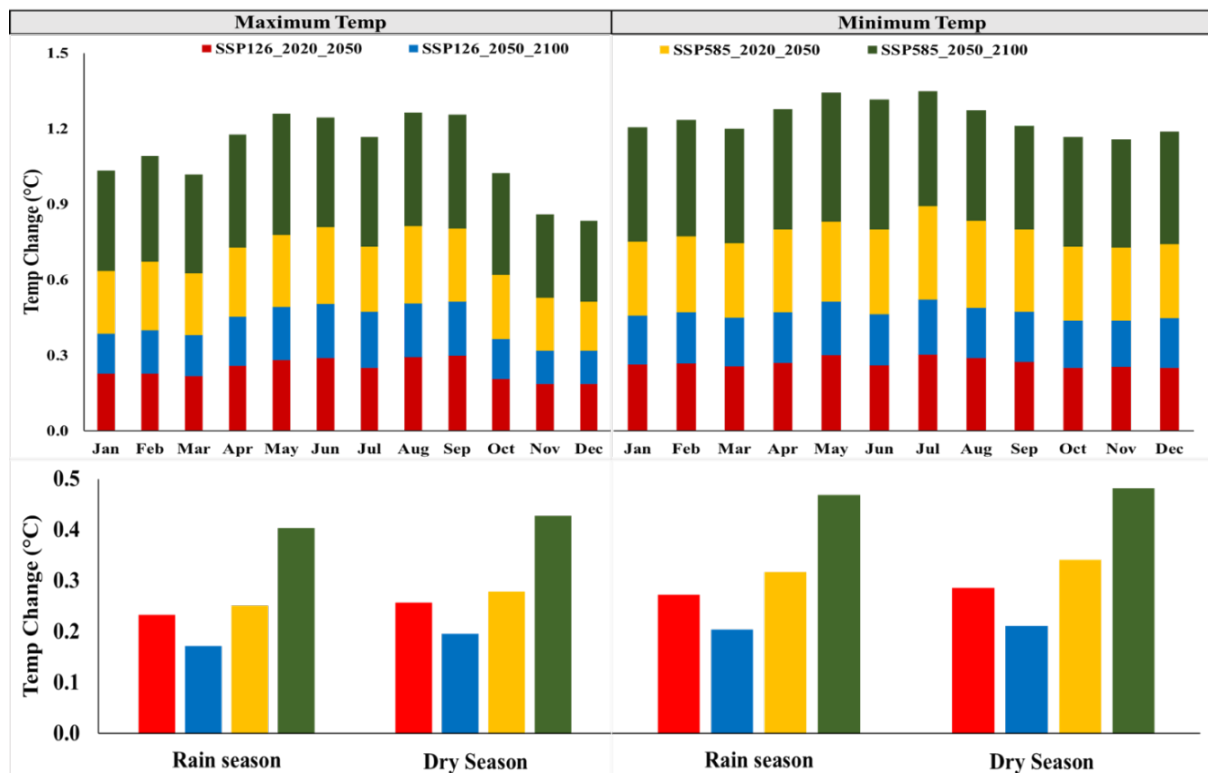


Figure 4. Absolute change in maximum and minimum temperatures; the upper plot shows monthly changes, while the lower plot shows seasonal changes.

3.2. Calibration and Validation of the SWAT Model

Based on the results of the sensitivity analysis performed by the SUFI-2 program using SWAT-CUP, the top four parameters were identified as the most sensitive for streamflow simulation, while the last three were slightly sensitive. To estimate the amount of flow from the catchment, the most sensitive flow prediction parameters (Table 1) were adjusted to suit the model simulations with the observed flow data. The comparison of monthly observed and simulated discharge throughout the calibration (January 2011 to December 2012) and validation (January 2013 to December 2013) periods demonstrated that the model was satisfactory for estimating the impacts of climate variability on the water balance across the study area, as revealed by model performance statistical measures, including the coefficient of determination (R^2), the Nash–Sutcliffe efficiency (NSE), and the relative error (RE). In line with a recent study [7], the association between the observed and simulated flow (Figure 5) was computed using the above most common metrics for both calibration and validation processes. For example, R^2 and NSE presented good results (0.91% and 0.73%) and (0.86% and 0.70%) for both calibration and validation, respectively. Moreover, lower acceptable RE percentages (8.3% and 10.9%) were also obtained for calibration and validation, respectively. The obtained REs were found to be in conjunction with the national

criteria for flow prediction in China, indicating that a hydrological model can be considered effective when the relative error percentage of the simulated data is less than 20% [67].

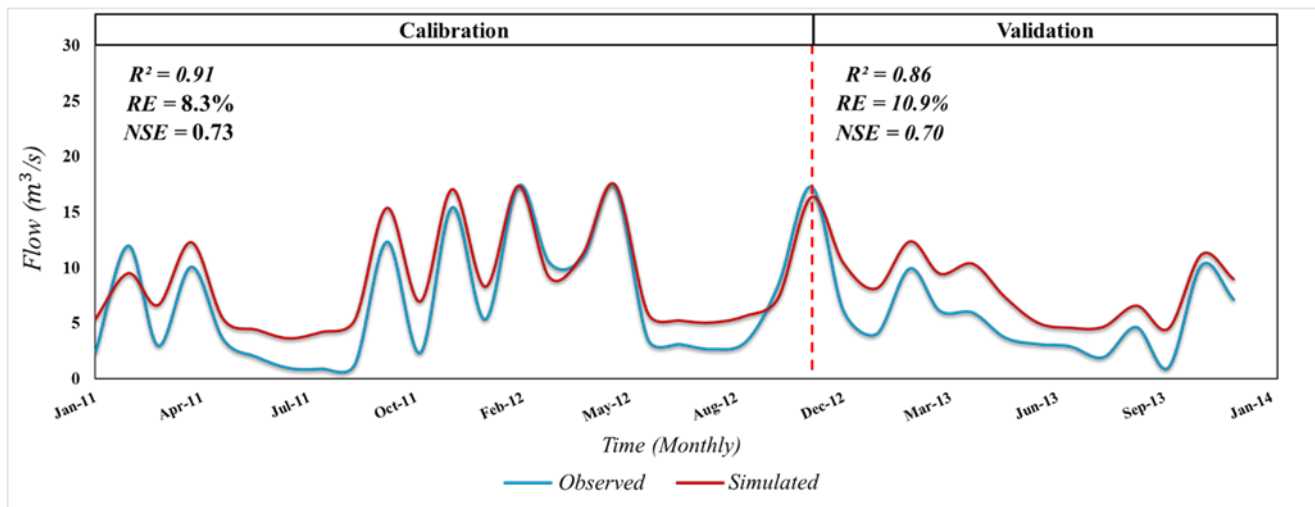


Figure 5. Observed and simulated streamflow during the calibration and validation.

3.3. Impact of Climate Change on Evapotranspiration

The average annual evapotranspiration (ET) over the entire catchment is expected to increase by 18.02 (17.41%) for SSP126 in the 2020–2050 (2050–2100) period, while under SSP585 an increase of 18.90 (21.78%) is expected in 2020–2050 (2050–2100). The projected monthly evapotranspiration (Figure 6a) was characterized by both increases and decreases under both scenarios and periods. On a monthly scale, a large decrease is more pronounced in March (34.97 to 0.43%), June (31.57 to 9.35%), and July (30.49 to 18.89%), while in February and December, an increase from 51.34 to 92.48% and from 37.52 to 88.29% is projected under both scenarios and periods, respectively. On a seasonal scale (Figure 6b), ET is projected to increase more during the rain season compared to the dry season. In the OND season (Figure 6c), a greater increase in ET is projected due to a projected increase in precipitation and temperature while, the MAM season will experience a decrease and a less significant increase under both scenarios. These findings are consistent with those of Mishra, et al. [68], who reported that the increased rainfall and temperature would result in increased ET. Throughout the projection periods, there will be a generally positive trend in ET owing to the expected rise in temperature as a result of global warming [12,69]. Moreover, Dai, et al. [70] evaluated the relationship between the Palmer Drought Index and soil moisture, as well as the effects of surface heat, concluding that the probability of drought will rise as anthropogenic global warming progresses due to higher temperatures and increased drying. Several studies [48,61,71] have also reported an increase in temperature across the African tropics. Furthermore, Nooni, et al. [72] reported that humid tropical and equatorial zones are expected to experience a significant increase in ET, especially in central and eastern Africa. Under SSP126 from June to August (the long dry season), a projected monthly increase in temperature of $0.28 \text{ }^\circ\text{C decade}^{-1}$ and a decrease in precipitation of 2.52% resulted in an ET decrease of 18.61% during 2020–2050. Furthermore, due to the increase in temperature and decrease in precipitation, evaporation has decreased significantly during the dry season. Situations such as increases in temperature and declines in precipitation can have negative impacts on soil moisture [73]. Soil moisture depletion will reduce catchment water availability, resulting in a decrease in expected ET. In fact, the soil's lack of water for evaporation due to the aridity (dryness) of the soil decreases the soil moisture by decreasing the water content in the soil, thus reducing the evaporation [73]. To explain the above, climate change and its related global warming may lead to increased surface dryness and more droughts owing to decreased precipitation, especially in the tropical regions. This is consistent with previous results [43] indicating

that increasing temperature leads to reduced soil moisture content which, in turn, leads to low crop productivity. A recent study showed the vulnerability of crop productivity in Rwanda to climate variability [21]. Furthermore, the study by Li, et al. [74] noted that 83% of the transferred forestland was converted to cultivated land after 2010, which will have a significant influence on the hydrological process. As also reported by a previous study [40], all of these may lead to a decline in surface runoff in the study area.

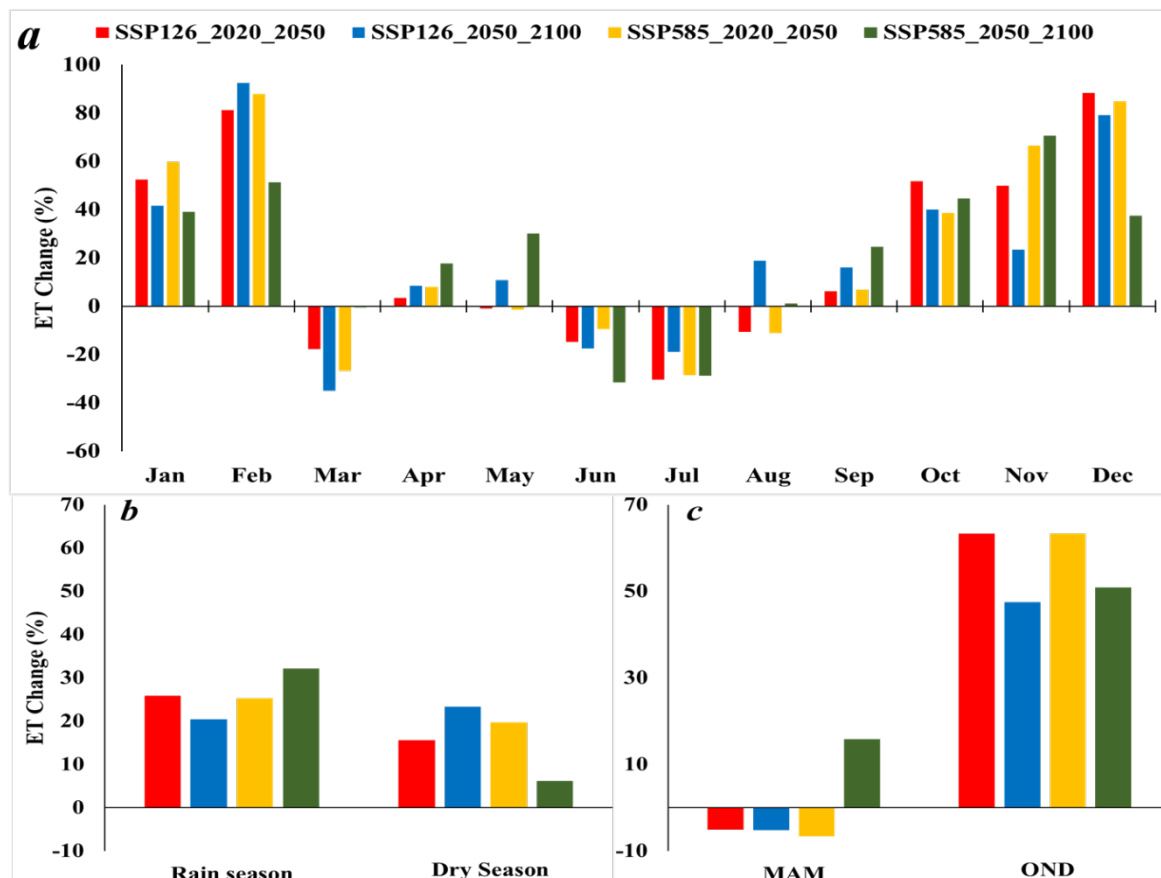


Figure 6. Relative evapotranspiration changes: (a) monthly, (b) seasonal, and (c) in rainy seasons.

3.4. Streamflow under Climate Change

The average annual discharge is projected to decrease by 7.2 and 3.49% under SSP126 in 2020–2050 and 2050–2100, respectively. Under SSP585, streamflow simulations indicate a 3.26% increase in 2020–2050 and a 4.53% decline in 2050–2100. On a monthly scale (Figure 7a), the largest decrease in average flows compared to the baseline period was projected to occur in June (36.95%) for the period 2020–2050 under the SSP126 scenario. The largest increase was projected in July, at 34.12% for the period 2020–2050 under the SSP585 scenario. High evapotranspiration due to the increase in temperature may be the source of the reverse trends of precipitation and streamflow in the rainy seasons (Figure 7b) [75,76]. A decrease in discharge projected in June is linked to a decline in projected rainfall in both scenarios and periods. The results show that in a future climate, the relationship between streamflow and precipitation may change, with a unit decrease in precipitation leading to a greater decrease in streamflow in the middle and late centuries, and vice versa. In agreement with previous findings [77,78], streamflow projections based on RCP climate scenarios show a decline in streamflow due to decreasing precipitation and rising temperature in East Africa. As a result, any change in precipitation will have a substantial impact on the flow of the watershed, which will be noticeable in both scenarios and periods. The relative changes in the projected low flow (Figure 7c) are projected to

decrease by 63.38 (24.8)% under SSP126 (SSP585) in the 2020–2050 period, while in the period 2050–2100, an increase of 20.33 and 2.74% is expected under SSP126 and SSP585, respectively. The relative changes in the projected peak flow indicate that the flow will be increase by 5.89 (11.46)% under SSP585 in the 2020–2050 (2050–2100) period, while under SSP126 it will decrease by 0.72% in the 2020–2050 period and increase by 1.73% in the 2050–2100 period. The increase in peak flow rate is encountered more under SSP585 than SSP126. These results correspond to the findings of Peter, et al. [79], who reported that the flow out of the Nyabugogo catchment is projected to decrease considerably in the future, reaching average flows of 50% compared to the current situation. Particularly low flows during dry months are expected to decrease by ~60%. This is in accordance with the findings of [76,80], which reported that the percentage of the change in low flow is greater than that in high flow, and that the increasing rates of high flow are more serious under RCP8.5 than under RCP2.6 and RCP4.5. The predicted streamflow trend corresponds to variations and trends in precipitation and evapotranspiration [48,81]. These findings are consistent with the growing evidence that the world is warming. Based on current precipitation patterns, studies [76,82] have shown that higher temperatures cause increased evaporation rates, which reduce streamflow and increase the frequency of droughts. This will almost certainly have a negative impact on the catchment’s agricultural productivity and irrigation management.

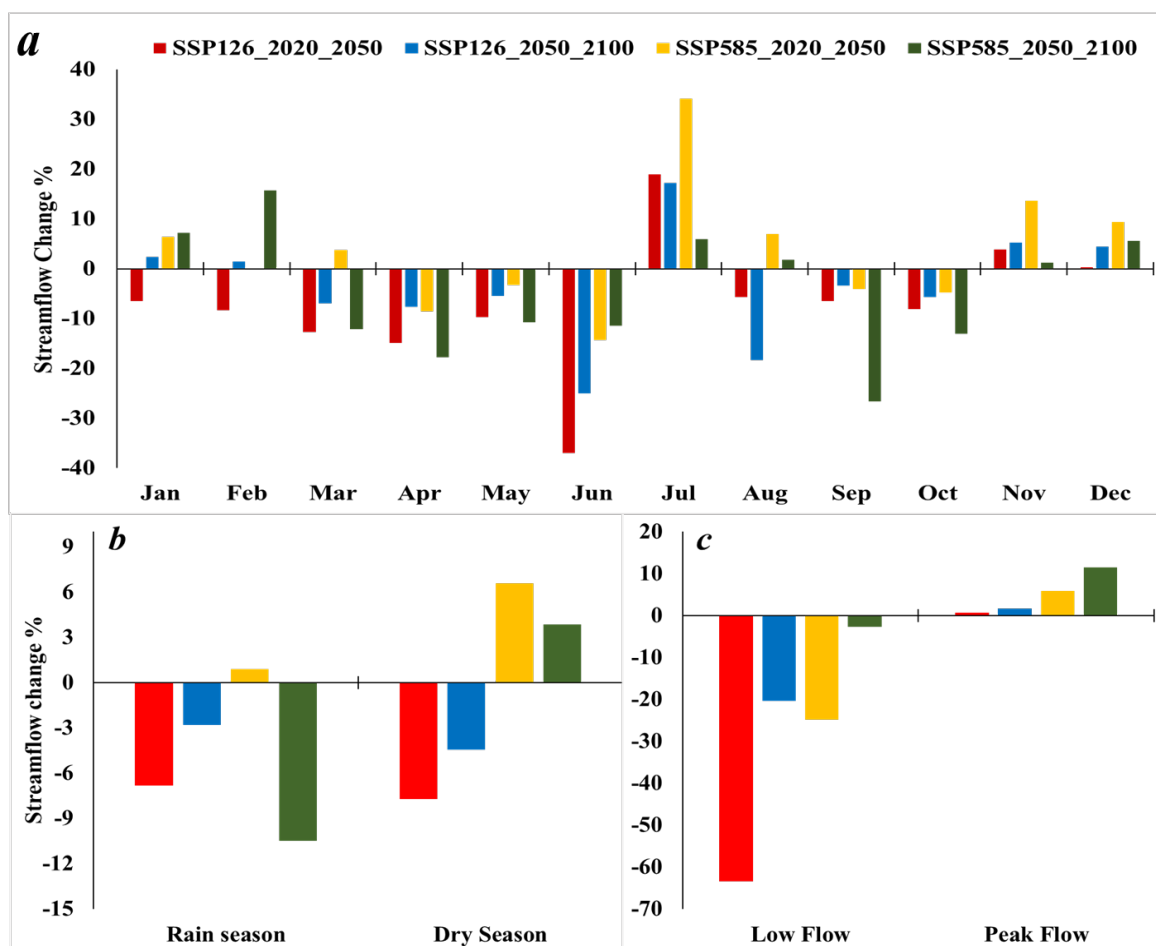


Figure 7. Relative streamflow changes: (a) monthly, (b) seasonal, and (c) in low and peak flow.

3.5. Surface Runoff under Climate Change

Surface runoff is strongly related to temperature and precipitation [67]. Climate change is projected to impact water resources and the related sectors—such as agriculture,

household consumption, and energy formation—in the Nyabugogo catchment as a result of decreased precipitation and increased temperatures. The average annual surface runoff of the basin is projected to decrease by 11.66 (4.40)% under SSP126 in the 2020–2050 (2050–2100) period, while an increase of 3.25% is expected under SSP585 in 2020–2050, followed by a decline of 5.42% in 2050–2100. According to the results, monthly runoff decreased by more than 20% due to a slight increase in precipitation and a continued increase in evapotranspiration. On the monthly scale (Figure 8a), a high decrease is expected in April (−34.23 to −7.21%), May (−28.99 to −5.65%), and June (−43.62 to −13.31%) under both SSP scenarios and periods. A decrease in surface runoff of 43.62 (33.27) % in June could be attributed to a decrease in rainfall of 8.96 (1.27) % and an increase in temperature of 2.43 (1.82) °C under SSP126 in 2020–2050 (2050–2100). In line with the findings of [77], the expected increase or decrease in surface runoff was related to future increases or decreases in precipitation and temperature across the basin. A decrease in runoff is expected in both dry and rainy seasons (Figure 8b), except under SSP585 in the period 2020–2050. During the rainy season (Figure 8c), less significant increases and decreases in precipitation were projected under SSP126 in both periods, which should result in increased runoff. However, a decrease was predicted, which could be associated with a significant increase in ET due to increased maximum and minimum temperatures [27,83]. Temperature effects tend to dominate in the 21st century under the high-emissions scenario, which had a significant impact on reducing runoff despite the predicted increase in precipitation during the rainy season [84,85]. This will aggravate water scarcity, increase water demand, and lead to further water scarcity in the study area. Due to the significant decrease in surface runoff, the irrigation water requirements will increase as well. Apart from climate change, population growth and changes in agricultural and industrial demand will also have significant impacts on the surface runoff in the future.

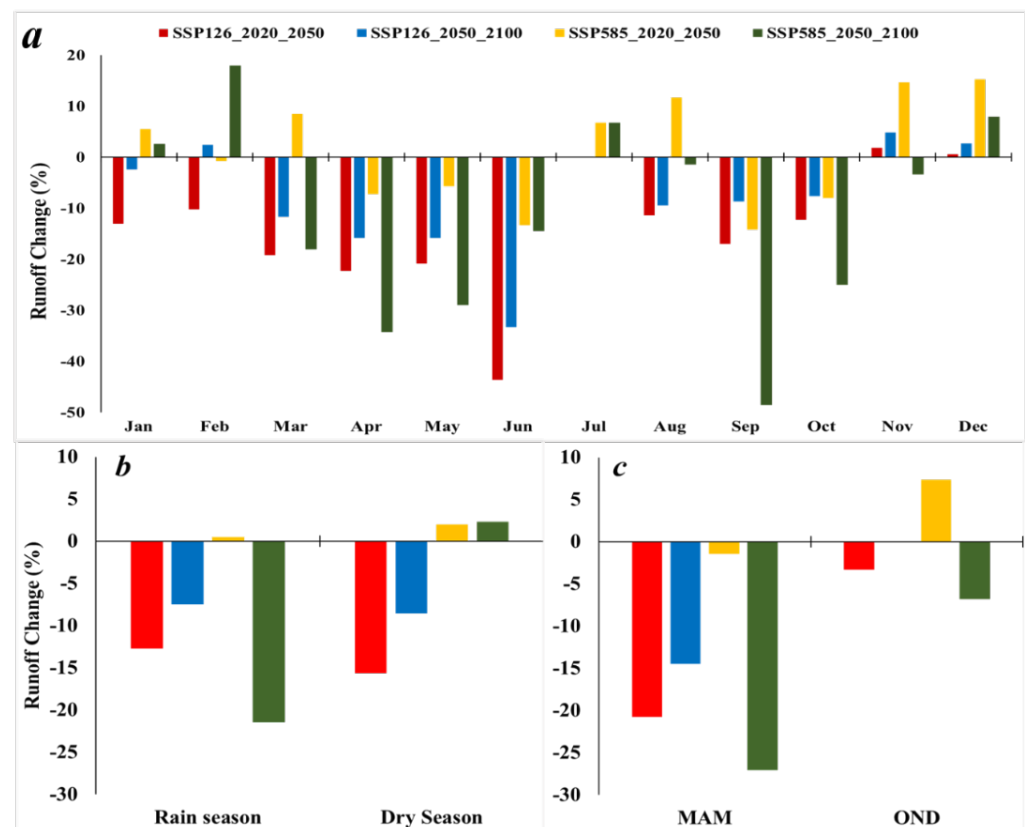


Figure 8. Relative runoff changes: (a) monthly, (b) seasonal, and (c) in rainy seasons.

3.6. Limitations of the Study

The use of hydrological models to study the impact of climate change on streamflow incorporates a range of uncertainties [86,87]. The most significant sources of uncertainty in climate change studies are the selection of the GCM models and the emission scenario specifications [86,88]. In the regional climate change research, the divergence between different GCM models is commonly regarded as a substantial source of uncertainty [89,90]. Due to differences in spatial domains and predictor factors, there may be a considerable difference in future climate data when downscaling with dynamic and statistical downscaling approaches [91]. Since the study used the same LCLU data, another source of uncertainty could be the impact of future changes in land use and soil parameters (which could influence soil properties in the watershed). Several parameters, such as LCLU, can have an impact on hydrology, since changes in LCLU alter river flow by modifying the evapotranspiration regime [92]. Due to the downscaling, hydrological parameter uncertainty, and neglect of the changes in land use and soil properties, there is a mixture of uncertainties in the GCMs' outputs. Any or all of these parameters could cause the results to differ from reality. Despite its limitations, this study aimed to analyze the probable effects of climate change on the water balance in the Nyabugogo catchment in Rwanda by seeking the best available data and utilizing the most feasible possible emission scenarios to reduce the uncertainty of the model predictions.

4. Conclusions

This study attempted to simulate the near- and far-future behavior of water balance conditions across the Nyabugogo catchment area using climate change simulations performed by 10 GCMs that contributed to CMIP6. The effects of climate change on streamflow, runoff, and evapotranspiration were also evaluated for both historical and future periods. The outcomes of the study showed a slight significant increase in precipitation and a remarkable significant ($p < 0.05$) increase in both maximum and minimum temperature; which showed an impact on the evapotranspiration in the catchment area. The streamflow was projected to decrease by 7.2 (3.49)% under SSP126 in the 2020–2050 (2050–2100) period; under SSP585, it showed a 3.26% increase in 2020–2050 and a 4.53% decline in 2050–2100. The average annual surface runoff was also projected to decrease by 11.66 (4.40)% under SSP126 in the 2020–2050 (2050–2100) period, while under SSP585 an increase of 3.25% in 2020–2050 and a decline of 5.42% in 2050–2100 was expected. In conclusion, the projected reductions in streamflow and runoff might imply an increased demand for irrigation, which may intensify the water stress in the study area under the future climate scenarios and, therefore, affect food and water security in the region. The findings of this study illuminate the probability of future water consensus, and can assist with future development strategies to balance water demand and supply. These findings can, therefore, be incorporated into water resource management plans in order to promote more sustainable water use in the catchment area. Although the common understanding reveals the vulnerability of this area to climate change, studies on the impact of future climate change on the water balance of this region are still scarce. However, in order to obtain a more comprehensive assessment and guide the development of adaptation strategies, future research should take into account the impact of changes in LCLU and soil parameters on water balance, so as to lessen the detrimental impact of climate change on agriculture and other industries.

Author Contributions: Conceptualization, A.U. (Adeline Umugwaneza), T.L., E.D.U., R.I. and A.U. (Aline Uwineza); methodology, A.U. (Adeline Umugwaneza), T.L.; software, A.U. (Adeline Umugwaneza) and Z.L.; validation, A.U. (Adeline Umugwaneza); formal analysis, A.U. (Adeline Umugwaneza), S.U.; investigation and resources, A.U. (Adeline Umugwaneza) and S.U.; data curation, A.U. (Adeline Umugwaneza) and Z.L.; writing—original draft preparation, A.U. (Adeline Umugwaneza), R.M. and E.D.U.; writing—review and editing, A.U. (Adeline Umugwaneza) and R.M.; visualization, A.U. (Adeline Umugwaneza) and R.I.; supervision, T.L.; project administration, and funding acquisition, X.C. and T.L. All authors have read and agreed to the published version of the manuscript.

Funding: This study was supported by the Strategic Priority Research Program of the Chinese Academy of Sciences, the Pan-Third Pole Environment Study for a Green Silk Road (Grant No. XDA20060303), the International Cooperation Project of the National Natural Science Foundation of China (Grant No. 41761144079), the project of the Research Center for Ecology and Environment of Central Asia (Grant No. Y934031), the Regional Collaborative Innovation Project of Xinjiang Uygur Autonomous Regions (Grant No. 2020E01010), and the KC Wong Education Foundation (GJTD-2020-14). A special acknowledgment should be expressed to the China–Pakistan Joint Research Center on Earth Sciences, who supported the implementation of this study.

Institutional Review Board Statement: Not applicable.

Informed Consent Statement: Not applicable.

Data Availability Statement: The source of all the data used in this study is provided in the manuscript.

Acknowledgments: The authors express sincere gratitude to the Rwanda Natural Resources Authority and the Rwanda Meteorological Agency for the provision of data. Additionally, the authors greatly acknowledge the support received from the Xinjiang Institute of Ecology and Geography, Chinese Academy of Sciences (CAS).

Conflicts of Interest: All authors declare no conflict of interest.

References

- Adhikari, U.; Nejadhashemi, A.P.; Herman, M.R. A review of climate change impacts on water resources in East Africa. *Trans. ASABE* **2015**, *58*, 1493–1507.
- Wu, J. Landscape sustainability science: Ecosystem services and human well-being in changing landscapes. *Landscape Ecol.* **2013**, *28*, 999–1023. [[CrossRef](#)]
- Brown, M.E.; Funk, C.C. *Food Security under Climate Change*; Nasa Publications, NASA: Washington, DC, USA, 2008.
- Haile, G.G.; Tang, Q.; Leng, G.; Jia, G.; Wang, J.; Cai, D.; Sun, S.; Baniya, B.; Zhang, Q. Long-term spatiotemporal variation of drought patterns over the Greater Horn of Africa. *Sci. Total Environ.* **2020**, *704*, 135299. [[CrossRef](#)]
- Ficklin, D.L.; Stewart, I.T.; Maurer, E.P. Effects of projected climate change on the hydrology in the Mono Lake Basin, California. *Clim. Chang.* **2013**, *116*, 111–131. [[CrossRef](#)]
- Reshmidevi, T.; Kumar, D.N.; Mehrotra, R.; Sharma, A. Estimation of the climate change impact on a catchment water balance using an ensemble of GCMs. *J. Hydrol.* **2018**, *556*, 1192–1204. [[CrossRef](#)]
- Mind’je, R.; Li, L.; Kayumba, P.M.; Mindje, M.; Ali, S.; Umugwaneza, A. Integrated Geospatial Analysis and Hydrological Modeling for Peak Flow and Volume Simulation in Rwanda. *Water* **2021**, *13*, 2926. [[CrossRef](#)]
- McCabe, G.J.; Wolock, D.M. Independent effects of temperature and precipitation on modeled runoff in the conterminous United States. *Water Resour. Res.* **2011**, *47*, 2. [[CrossRef](#)]
- Buytaert, W.; Célleri, R.; Timbe, L. Predicting climate change impacts on water resources in the tropical Andes: Effects of GCM uncertainty. *Geophys. Res. Lett.* **2009**, *36*, 7. [[CrossRef](#)]
- Worqlul, A.W.; Dile, Y.T.; Ayana, E.K.; Jeong, J.; Adem, A.A.; Gerik, T. Impact of climate change on streamflow hydrology in headwater catchments of the Upper Blue Nile Basin, Ethiopia. *Water* **2018**, *10*, 120. [[CrossRef](#)]
- Asadieh, B.; Krakauer, N.Y. Global change in streamflow extremes under climate change over the 21st century. *Hydrol. Earth Syst. Sci.* **2017**, *21*, 5863–5874. [[CrossRef](#)]
- IPCC. *Climate Change 2014: Impacts, Adaptation, and Vulnerability. Part B: Regional Aspects. Contribution of Working Group II to the Fifth Assessment Report of the Intergovernmental Panel on Climate Change 2014*; IPCC: Geneva, Switzerland, 2014.
- IPCC. *Climate Change 2007—Impacts, Adaptation and Vulnerability: Working Group II Contribution to the Fourth Assessment Report of the IPCC*; Cambridge University Press: Cambridge, UK, 2007; Volume 4.
- Gebrechorkos, S.H.; Hülsmann, S.; Bernhofer, C. Regional climate projections for impact assessment studies in East Africa. *Environ. Res. Lett.* **2019**, *14*, 044031. [[CrossRef](#)]
- Rippke, U.; Ramirez-Villegas, J.; Jarvis, A.; Vermeulen, S.J.; Parker, L.; Mer, F.; Diekkrueger, B.; Challinor, A.J.; Howden, M. Timescales of transformational climate change adaptation in sub-Saharan African agriculture. *Nat. Clim. Chang.* **2016**, *6*, 605–609. [[CrossRef](#)]
- Adhikari, U.; Nejadhashemi, A.P.; Woznicki, S.A. Climate change and eastern Africa: A review of impact on major crops. *Food Energy Secur.* **2015**, *4*, 110–132. [[CrossRef](#)]
- Ngoma, H.; Wen, W.; Ojara, M.; Ayugi, B. Assessing current and future spatiotemporal precipitation variability and trends over Uganda, East Africa, based on CHIRPS and regional climate model datasets. *Meteorol. Atmos. Phys.* **2021**, *133*, 823–843. [[CrossRef](#)]
- Hulme, M.; Doherty, R.; Ngara, T.; New, M.; Lister, D. African climate change: 1900–2100. *Clim. Res.* **2001**, *17*, 145–168. [[CrossRef](#)]
- Haggag, M.; Kalisa, J.C.; Abdeldayem, A.W. Projections of precipitation, air temperature and potential evapotranspiration in Rwanda under changing climate conditions. *Afr. J. Environ. Sci. Technol.* **2016**, *10*, 18–33.

20. Asumadu-Sarkodie, S.; Rufangura, P.; Jayaweera, M.; Owusu, P.A. Situational analysis of flood and drought in Rwanda. *Int. J. Sci. Eng. Res.* **2017**, *6*, 960–970. [[CrossRef](#)]
21. Austin, K.G.; Beach, R.H.; Lapidus, D.; Salem, M.E.; Taylor, N.J.; Knudsen, M.; Ujeneza, N. Impacts of Climate Change on the Potential Productivity of Eleven Staple Crops in Rwanda. *Sustainability* **2020**, *12*, 4116. [[CrossRef](#)]
22. Umuhoza, J.; Chen, L.; Mumo, L. Assessing the skills of rossby centre regional climate model in simulating observed rainfall over Rwanda. *Atmos. Clim. Chang.* **2021**, *11*, 398–418. [[CrossRef](#)]
23. Gelete, G.; Gokcekus, H.; Gichamo, T. Impact of climate change on the hydrology of Blue Nile basin, Ethiopia: A review. *J. Water Clim. Chang.* **2020**, *11*, 1539–1550. [[CrossRef](#)]
24. Huang, Y.; Chen, X.; Li, Y.; Willems, P.; Liu, T. Integrated modeling system for water resources management of Tarim River Basin. *Environ. Eng. Sci.* **2010**, *27*, 255–269. [[CrossRef](#)]
25. Huang, Y.; Ma, Y.; Liu, T.; Luo, M. Climate change impacts on extreme flows under IPCC RCP scenarios in the mountainous Kaidu watershed, Tarim River basin. *Sustainability* **2020**, *12*, 2090. [[CrossRef](#)]
26. Li, C.; Fang, H. Assessment of climate change impacts on the streamflow for the Mun River in the Mekong Basin, Southeast Asia: Using SWAT model. *CATENA* **2021**, *201*, 105199. [[CrossRef](#)]
27. Rabezanahary Tantelinaiaina, M.F.; Rahaman, M.H.; Zhai, J. Assessment of the Future Impact of Climate Change on the Hydrology of the Mangoky River, Madagascar Using ANN and SWAT. *Water* **2021**, *13*, 1239. [[CrossRef](#)]
28. O'Neill, B.C.; Kriegler, E.; Ebi, K.L.; Kemp-Benedict, E.; Riahi, K.; Rothman, D.S.; van Ruijven, B.J.; van Vuuren, D.P.; Birkmann, J.; Kok, K. The roads ahead: Narratives for shared socioeconomic pathways describing world futures in the 21st century. *Glob. Environ. Chang.* **2017**, *42*, 169–180. [[CrossRef](#)]
29. Manyifika, M. Diagnostic Assessment on Urban Floods Using Satellite Data and Hydrologic Models in Kigali, Rwanda. Master's Thesis, University of Twente, Twente, The Netherlands, 2015; pp. 23–25.
30. Government of Rwanda (NISR, M.o.E.). *Natural Capital Accounts for Water*; Government of Rwanda: Kigali, Rwanda, 2019.
31. Musoni, J.; Wali, U.; Munyaneza, O. Runoff coefficient classification on Nyabugogo catchment. In Proceedings of the Hydrology, 10th International WaterNet/WARFSA/GWP-SA Symposium, Entebbe, Uganda, 28–30 October 2009.
32. Munyaneza, O.; Nzeyimana, Y.K.; Wali, U.G. Hydraulic Structures Design for Flood Control in the Nyabugogo Wetland, Rwanda. *Nile Basin Water Sci. Eng. J.* **2013**, *6*, 26–37.
33. Umwali, E.D.; Kurban, A.; Isabwe, A.; Mind'je, R.; Azadi, H.; Guo, Z.; Udahogora, M.; Nyirarwasa, A.; Umuhoza, J.; Nzabarinda, V. Spatio-seasonal variation of water quality influenced by land use and land cover in Lake Muhazi. *Sci. Rep.* **2021**, *11*, 17376. [[CrossRef](#)]
34. Krysanova, V.; White, M. Advances in water resources assessment with SWAT—An overview. *Hydrol. Sci. J.* **2015**, *60*, 771–783. [[CrossRef](#)]
35. Arnold, J.G.; Srinivasan, R.; Muttiah, R.S.; Williams, J.R. Large area hydrologic modeling and assessment part I: Model development 1. *J. Am. Water Resour. Assoc.* **1998**, *34*, 73–89. [[CrossRef](#)]
36. Gabiri, G.; Diekkrüger, B.; Näschen, K.; Leemhuis, C.; van der Linden, R.; Majaliwa, J.-G.M.; Obando, J.A. Impact of Climate and Land Use/Land Cover Change on the Water Resources of a Tropical Inland Valley Catchment in Uganda, East Africa. *Climate* **2020**, *8*, 83. [[CrossRef](#)]
37. Tegegne, G.; Park, D.K.; Kim, Y.-O. Comparison of hydrological models for the assessment of water resources in a data-scarce region, the Upper Blue Nile River Basin. *J. Hydrol. Reg. Stud.* **2017**, *14*, 49–66. [[CrossRef](#)]
38. USDA. *National Engineering Handbook, Section 4: Hydrology*; USDA: Washington, DC, USA, 1972.
39. Hargreaves, G.H.; Samani, Z.A. Reference crop evapotranspiration from temperature. *Appl. Eng. Agric.* **1985**, *1*, 96–99. [[CrossRef](#)]
40. Setegn, S.G.; Rayner, D.; Melesse, A.M.; Dargahi, B.; Srinivasan, R. Impact of climate change on the hydroclimatology of Lake Tana Basin, Ethiopia. *Water Resour. Res.* **2011**, *47*, W04511. [[CrossRef](#)]
41. Polanco, E.I.; Fleifle, A.; Ludwig, R.; Disse, M. Improving SWAT model performance in the upper Blue Nile Basin using meteorological data integration and subcatchment discretization. *Hydrol. Earth Syst. Sci.* **2017**, *21*, 4907–4926. [[CrossRef](#)]
42. Samadi, S.Z. Assessing the sensitivity of SWAT physical parameters to potential evapotranspiration estimation methods over a coastal plain watershed in the southeastern United States. *Hydrol. Res.* **2016**, *48*, 395–415. [[CrossRef](#)]
43. Abbaspour, K.C.; Johnson, C.; van Genuchten, M.T. Estimating uncertain flow and transport parameters using a sequential uncertainty fitting procedure. *Vadose Zone J.* **2004**, *3*, 1340–1352. [[CrossRef](#)]
44. Zettam, A.; Taleb, A.; Sauvage, S.; Boithias, L.; Belaidi, N.; Sánchez-Pérez, J.M. Modelling hydrology and sediment transport in a semi-arid and anthropized catchment using the SWAT model: The case of the Tafna river (northwest Algeria). *Water* **2017**, *9*, 216. [[CrossRef](#)]
45. Riahi, K.; Van Vuuren, D.P.; Kriegler, E.; Edmonds, J.; O'Neill, B.C.; Fujimori, S.; Bauer, N.; Calvin, K.; Dellink, R.; Fricko, O. The Shared Socioeconomic Pathways and their energy, land use, and greenhouse gas emissions implications: An overview. *Glob. Environ. Chang.* **2017**, *42*, 153–168. [[CrossRef](#)]
46. Dosio, A.; Jury, M.W.; Almazroui, M.; Ashfaq, M.; Diallo, I.; Engelbrecht, F.A.; Klutse, N.A.; Lennard, C.; Pinto, I.; Sylla, M.B. Projected future daily characteristics of African precipitation based on global (CMIP5, CMIP6) and regional (CORDEX, CORDEX-CORE) climate models. *Clim. Dyn.* **2021**, *57*, 3135–3158. [[CrossRef](#)]
47. Ayugi, B.; Dike, V.; Ngoma, H.; Babaoumail, H.; Mumo, R.; Ongoma, V. Future Changes in Precipitation Extremes over East Africa Based on CMIP6 Models. *Water* **2021**, *13*, 2358. [[CrossRef](#)]

48. Onyutha, C.; Asimwe, A.; Ayugi, B.; Ngoma, H.; Ongoma, V.; Tabari, H. Observed and Future Precipitation and Evapotranspiration in Water Management Zones of Uganda: CMIP6 Projections. *Atmosphere* **2021**, *12*, 887. [[CrossRef](#)]
49. Liu, J.; Liu, T.; Bao, A.; De Maeyer, P.; Feng, X.; Miller, S.N.; Chen, X. Assessment of different modelling studies on the spatial hydrological processes in an arid alpine catchment. *Water Resour. Manag.* **2016**, *30*, 1757–1770. [[CrossRef](#)]
50. Bi, D.; Dix, M.; Marsland, S.; Hirst, T.; O'Farrell, S.; Uotila, P.; Sullivan, A.; Yan, H.; Kowalczyk, E.; Rashid, H. ACCESS: The Australian coupled climate model for IPCC AR5 and CMIP5. In *Climate Change Beijing*; Chinese Academy of Science: Beijing, China, 2012.
51. Law, R.M.; Ziehn, T.; Matear, R.J.; Lenton, A.; Chamberlain, M.A.; Stevens, L.E.; Wang, Y.-P.; Srbinovsky, J.; Bi, D.; Yan, H. The carbon cycle in the Australian Community Climate and Earth System Simulator (ACCESS-ESM1)–Part 1: Model description and pre-industrial simulation. *Geosci. Model Dev.* **2017**, *10*, 2567–2590. [[CrossRef](#)]
52. Voldoire, A.; Saint-Martin, D.; S en esi, S.; Decharme, B.; Alias, A.; Chevallier, M.; Colin, J.; Gu er emy, J.F.; Michou, M.; Moine, M.P. Evaluation of CMIP6 deck experiments with CNRM-CM6-1. *J. Adv. Modeling Earth Syst.* **2019**, *11*, 2177–2213. [[CrossRef](#)]
53. S ef erian, R.; Nabat, P.; Michou, M.; Saint-Martin, D.; Voldoire, A.; Colin, J.; Decharme, B.; Delire, C.; Berthet, S.; Chevallier, M. Evaluation of CNRM earth system model, CNRM-ESM2-1: Role of earth system processes in present-day and future climate. *J. Adv. Model. Earth Syst.* **2019**, *11*, 4182–4227. [[CrossRef](#)]
54. Swart, N.C.; Cole, J.N.; Kharin, V.V.; Lazare, M.; Scinocca, J.F.; Gillett, N.P.; Anstey, J.; Arora, V.; Christian, J.R.; Hanna, S. The Canadian earth system model version 5 (CanESM5. 0.3). *Geosci. Model Dev.* **2019**, *12*, 4823–4873. [[CrossRef](#)]
55. Volodin, E.M.; Mortikov, E.V.; Kostykin, S.V.; Galin, V.Y.; Lykossov, V.N.; Gritsun, A.S.; Diansky, N.A.; Gusev, A.V.; Iakovlev, N.G.; Shestakova, A.A. Simulation of the modern climate using the INM-CM48 climate model. *Russ. J. Numer. Anal. Math. Model.* **2018**, *33*, 367–374. [[CrossRef](#)]
56. Boucher, O.; Servonnat, J.; Albright, A.L.; Aumont, O.; Balkanski, Y.; Bastrikov, V.; Bekki, S.; Bonnet, R.; Bony, S.; Bopp, L. Presentation and evaluation of the IPSL-CM6A-LR climate model. *J. Adv. Modeling Earth Syst.* **2020**, *12*, e2019MS002010. [[CrossRef](#)]
57. Tatebe, H.; Ogura, T.; Nitta, T.; Komuro, Y.; Ogochi, K.; Takemura, T.; Sudo, K.; Sekiguchi, M.; Abe, M.; Saito, F. Description and basic evaluation of simulated mean state, internal variability, and climate sensitivity in MIROC6. *Geosci. Model Dev.* **2019**, *12*, 2727–2765. [[CrossRef](#)]
58. Sellar, A.A.; Jones, C.G.; Mulcahy, J.P.; Tang, Y.; Yool, A.; Wiltshire, A.; O'connor, F.M.; Stringer, M.; Hill, R.; Palmieri, J. UKESM1: Description and evaluation of the UK Earth System Model. *J. Adv. Modeling Earth Syst.* **2019**, *11*, 4513–4558. [[CrossRef](#)]
59. Archibald, A.T.; O'Connor, F.M.; Abraham, N.L.; Archer-Nicholls, S.; Chipperfield, M.P.; Dalvi, M.; Folberth, G.A.; Dennison, F.; Dhomse, S.S.; Griffiths, P.T. Description and evaluation of the UKCA stratosphere–troposphere chemistry scheme (StratTrop vn 1.0) implemented in UKESM1. *Geosci. Model Dev.* **2020**, *13*, 1223–1266. [[CrossRef](#)]
60. Almazroui, M.; Saeed, F.; Saeed, S.; Islam, M.N.; Ismail, M.; Klutse, N.A.B.; Siddiqui, M.H. Projected change in temperature and precipitation over Africa from CMIP6. *Earth Syst. Environ.* **2020**, *4*, 455–475. [[CrossRef](#)]
61. Ongoma, V.; Chen, H.; Gao, C. Projected changes in mean rainfall and temperature over East Africa based on CMIP5 models. *Int. J. Climatol.* **2018**, *38*, 1375–1392. [[CrossRef](#)]
62. Ongoma, V.; Chen, H.; Omony, G.W. Variability of extreme weather events over the equatorial East Africa, a case study of rainfall in Kenya and Uganda. *Theor. Appl. Climatol.* **2018**, *131*, 295–308. [[CrossRef](#)]
63. Tan, G.; Ayugi, B.; Ngoma, H.; Ongoma, V. Projections of future meteorological drought events under representative concentration pathways (RCPs) of CMIP5 over Kenya, East Africa. *Atmos. Res.* **2020**, *246*, 105112. [[CrossRef](#)]
64. Gebrechorkos, S.H.; Bernhofer, C.; H ulsmann, S. Climate change impact assessment on the hydrology of a large river basin in Ethiopia using a local-scale climate modelling approach. *Sci. Total Environ.* **2020**, *742*, 140504. [[CrossRef](#)] [[PubMed](#)]
65. Michael, C. *Climate Change Impacts on East Africa a Review of the Scientific Literature*; WFF-World Wide Fund For Nature: Gland, Switzerland, 2006.
66. Engelbrecht, F.; Adegoke, J.; Bopape, M.-J.; Naidoo, M.; Garland, R.; Thatcher, M.; McGregor, J.; Katzfey, J.; Werner, M.; Ichoku, C. Projections of rapidly rising surface temperatures over Africa under low mitigation. *Environ. Res. Lett.* **2015**, *10*, 085004. [[CrossRef](#)]
67. Wang, J.; Hu, L.; Li, D.; Ren, M. Potential impacts of projected climate change under CMIP5 RCP scenarios on streamflow in the Wabash River Basin. *Adv. Meteorol.* **2020**, *2020*, 9698423. [[CrossRef](#)]
68. Mishra, V.; Lilhare, R. Hydrologic sensitivity of Indian sub-continental river basins to climate change. *Glob. Planet. Chang.* **2016**, *139*, 78–96. [[CrossRef](#)]
69. Swelam, A.; Jomaa, I.; Shapland, T.; Snyder, R.; Moratiel, R. Evapotranspiration Response to Climate Change. *Acta Hort.* **2011**, *922*, 91–98.
70. Dai, A.; Trenberth, K.E.; Qian, T. A global dataset of Palmer Drought Severity Index for 1870–2002: Relationship with soil moisture and effects of surface warming. *J. Hydrometeorol.* **2004**, *5*, 1117–1130. [[CrossRef](#)]
71. Iyakaremye, V.; Zeng, G.; Siebert, A.; Yang, X. Contribution of external forcings to the observed trend in surface temperature over Africa during 1901–2014 and its future projection from CMIP6 simulations. *Atmos. Res.* **2021**, *254*, 105512. [[CrossRef](#)]
72. Noon, I.K.; Hagan, D.F.T.; Wang, G.; Ullah, W.; Lu, J.; Li, S.; Dzakpasu, M.; Premph, N.A.; Lim, K.T. Future Changes in Simulated Evapotranspiration across Continental Africa Based on CMIP6 CNRM-CM6. *Int. J. Environ. Res. Public Health* **2021**, *18*, 6760. [[CrossRef](#)] [[PubMed](#)]

73. Dai, A.; Zhao, T.; Chen, J. Climate change and drought: A precipitation and evaporation perspective. *Curr. Clim. Chang. Rep.* **2018**, *4*, 301–312. [[CrossRef](#)]
74. Li, C.; Yang, M.; Li, Z.; Wang, B. How Will Rwandan Land Use/Land Cover Change under High Population Pressure and Changing Climate? *Appl. Sci.* **2021**, *11*, 5376. [[CrossRef](#)]
75. Getahun, Y.S.; van Lanen, I.H.; Torfs, P.P. Impact of Climate Change on Hydrology of the Upper Awash River Basin (Ethiopia): Inter-Comparison of Old SRES and New RCP Scenarios. Ph.D. Thesis, Wageningen University, Wageningen, The Netherlands, 2014.
76. Gurara, M.A.; Jilo, N.B.; Tolche, A.D. Modeling Climate Change Impact on the Streamflow in the Upper Wabe Bridge Watershed in Wabe Shebele River Basin, Ethiopia. *Int. J. River Basin Manag.* **2021**, 1–46. [[CrossRef](#)]
77. Daba, M.H.; You, S. Assessment of Climate Change Impacts on River Flow Regimes in the Upstream of Awash Basin, Ethiopia: Based on IPCC Fifth Assessment Report (AR5) Climate Change Scenarios. *Hydrology* **2020**, *7*, 98. [[CrossRef](#)]
78. Rowell, D.P.; Booth, B.B.; Nicholson, S.E.; Good, P. Reconciling past and future rainfall trends over East Africa. *J. Climate* **2015**, *28*, 9768–9788. [[CrossRef](#)]
79. Peter, D.; Maurits, K.; Froukje, D.B.; Wilco, T.; Mechteld, A.; Henk, P. *Water Balance and Allocation Modelling in Rwanda*; FutureWater: Wageningen, The Netherlands, 2017.
80. Oo, H.T.; Zin, W.W.; Kyi, C.T. Analysis of streamflow response to changing climate conditions using SWAT model. *Civ. Eng. J.* **2020**, *6*, 194–209. [[CrossRef](#)]
81. Tessema, N.; Kebede, A.; Yadeta, D. Modelling the effects of climate change on streamflow using climate and hydrological models: The case of the Kesem sub-basin of the Awash River basin, Ethiopia. *Int. J. River Basin Manag.* **2021**, *19*, 469–480. [[CrossRef](#)]
82. Tarekegn, N.; Abate, B.; Muluneh, A.; Dile, Y. Modeling the impact of climate change on the hydrology of Andasa watershed. *Modeling Earth Syst. Environ.* **2021**, 1–17. [[CrossRef](#)]
83. Bhatta, B.; Shrestha, S.; Shrestha, P.K.; Talchabhadel, R. Evaluation and application of a SWAT model to assess the climate change impact on the hydrology of the Himalayan River Basin. *CATENA* **2019**, *181*, 104082. [[CrossRef](#)]
84. Abraham, T.; Abate, B.; Woldemichael, A.; Muluneh, A. Impacts of Climate Change under CMIP5 RCP Scenarios on the Hydrology of Lake Ziway Catchment, Central Rift Valley of Ethiopia. *J. Environ. Earth Sci.* **2018**, *8*, 5.
85. Tshimanga, R.; Hughes, D. Climate change and impacts on the hydrology of the Congo Basin: The case of the northern sub-basins of the Oubangui and Sangha Rivers. *Phys. Chem. Earth* **2012**, *50*, 72–83. [[CrossRef](#)]
86. Thompson, J.; Green, A.; Kingston, D.; Gosling, S. Assessment of uncertainty in river flow projections for the Mekong River using multiple GCMs and hydrological models. *J. Hydrol.* **2013**, *486*, 1–30. [[CrossRef](#)]
87. Abdo, K.; Fiseha, B.; Rientjes, T.; Gieske, A.; Haile, A. Assessment of climate change impacts on the hydrology of Gilgel Abay catchment in Lake Tana basin, Ethiopia. *Hydrol. Process. Int. J.* **2009**, *23*, 3661–3669. [[CrossRef](#)]
88. Chen, J.; Brissette, F.P.; Poulin, A.; Leconte, R. Overall uncertainty study of the hydrological impacts of climate change for a Canadian watershed. *Water Resour. Res.* **2011**, *47*, 14. [[CrossRef](#)]
89. Wilby, R.L.; Dawson, C.W. The statistical downscaling model: Insights from one decade of application. *Int. J. Climatol.* **2013**, *33*, 1707–1719. [[CrossRef](#)]
90. Aich, V.; Liersch, S.; Vetter, T.; Huang, S.; Tecklenburg, J.; Hoffmann, P.; Koch, H.; Fournet, S.; Krysanova, V.; Müller, E. Comparing impacts of climate change on streamflow in four large African river basins. *Hydrol. Earth Syst. Sci.* **2014**, *18*, 1305–1321. [[CrossRef](#)]
91. Qiao, L.; Zou, C.B.; Gaitán, C.F.; Hong, Y.; McPherson, R.A. Analysis of precipitation projections over the climate gradient of the Arkansas Red River basin. *J. Appl. Meteorol. Climatol.* **2017**, *56*, 1325–1336. [[CrossRef](#)]
92. Näschen, K.; Diekkrüger, B.; Evers, M.; Höllermann, B.; Steinbach, S.; Thonfeld, F. The Impact of Land Use/Land Cover Change (LULCC) on Water Resources in a Tropical Catchment in Tanzania under Different Climate Change Scenarios. *Sustainability* **2019**, *11*, 7083. [[CrossRef](#)]